Propagation limits and velocity of reaction-diffusion fronts in a system of discrete random sources

Francois-David Tang, Andrew J. Higgins,* and Samuel Goroshin
McGill University, Department of Mechanical Engineering, Montreal, Quebec, Canada
(Received 12 October 2011; published 22 March 2012)

The effect of spatially randomizing a system of pointlike sources on the propagation of reaction-diffusion fronts is investigated in multidimensions. The dynamics of the reactive front are modeled by superimposing the solutions for diffusion from a single point source. A nondimensional parameter is introduced to quantify the discreteness of the system, based on the characteristic reaction time of sources compared to the diffusion time between sources. The limits to propagation and the average velocity of propagation are expressed as probabilistic quantities to account for the influence of the randomly distributed sources. In random systems, two- and three-dimensional fronts are able to propagate beyond a limit previously found for systems with regularly distributed sources, while a propagation limit in one dimension that is independent of domain size cannot be defined. The dimensionality of the system is seen to have a strong influence on the front propagation velocity, with higher dimensional systems propagating faster than lower dimensional systems. In a three-dimensional system, both the limit to propagation and average front velocity revert to a solution that assumes a spatially continuous source function as the discreteness parameter is increased to the continuum limit. The results indicate that reactive systems are able to exploit local fluctuations in source concentration to extend propagation limits and increase the velocity in comparison to regularly spaced systems.

DOI: 10.1103/PhysRevE.85.036311 PACS number(s): 47.70.−n, 05.40.−a, 82.40.Ck

I. INTRODUCTION

Diffusion of heat or a chemical species can propagate as a self-sustained front in a medium where the reaction rate is strongly dependent on the concentration of the diffusion component. In many cases, the reactive medium is heterogeneous and the sources generating the diffusive component are localized in space [1]. Condensed-phase systems capable of supporting self-propagating high-temperature synthesis (SHS) [2], forest fires in which combustion must propagate from tree to tree [3], and flames propagating in dust suspended in an oxidizing atmosphere [4] are all examples of reactive waves in systems with heterogeneous energy sources. In biological cells, the propagation of calcium waves via the self-induced release of calcium ions from localized receptors has been modeled as heterogeneous reaction-diffusion fronts [5–7]. In spite of the spatially discrete nature of the sources, the common approach in describing reactive-diffusion fronts in heterogeneous media is to introduce the source function in the governing diffusion equation as a continuous function of spatial coordinates [8,9].

As has been shown in recent work [4,7,10–12], homogenization of the source function is invalid when the characteristic length scales of the reaction-diffusion front are comparable with the scale of the heterogeneity through which it propagates. In this case, the position of the sources in the diffusion equation has to be described explicitly, and spatial homogenization of the source function cannot be justified. In the asymptotic case of pointlike sources and a stepwise reaction rate, a parameter τ_c defining the front propagation regime (continuum versus discrete) is given by the ratio of the characteristic reaction time t_r (duration of activity of the source) to the characteristic time required for the diffusion front to propagate through a distance l between the sources, $t_d = l^2/\alpha$ (where α is the diffusion coefficient and l is the average spacing between sources):

$$\tau_c = \frac{t_r}{t_d} = \frac{t_r \alpha}{l^2}. \tag{1}$$

When $\tau_c \gg 1$, the classical continuum approach is valid. In the other extreme (i.e., $\tau_c \to 0$), the front propagates in the discrete regime that has a number of unusual features in comparison to the properties of the classical continuum theory [4,7]. The front speed in the discrete regime is a weak function of the reaction time but is an explicit function of the distance between sources and their position (spatial distribution). Furthermore, a regular distribution of the sources as the nodes of a regular lattice leads to the appearance of a new propagation limit that cannot be predicted *a priori* from the system thermodynamics nor from the classical continuous reaction-diffusion theory [11,13]. Propagation beyond this limit is only possible in a system containing randomly distributed sources through local concentration fluctuations. The behavior of diffusion fronts in such systems is unavoidably statistical and requires a probabilistic approach for the description of both the front speed and the propagation limit.

II. OBJECTIVE AND APPROACH

The objective of the present paper is to investigate the statistical nature of reaction-diffusion fronts propagating in systems of spatially random sources as a function of the system dimensionality and the degree of discreteness. A methodology is developed to identify the fundamental propagation limit in systems with spatially random sources that is independent of the size of the domain and the conditions used to initiate the front. Specifically, numerical simulations in finite-sized domains are used in order to identify a limit that is expected to apply as the domain size tends to infinity and careful attention is paid to isolating the influence of the technique used to initiate the front in the simulations. The average front

*andrew.higgins@mcgill.ca

propagation velocity is also measured from these simulations and the results are compared to the predictions of the classical continuum solution and the solution for a system of regularly spaced sources.

III. REVIEW OF MODELS WITH CONTINUOUS OR REGULARLY SPACED DISCRETE SOURCES

Propagating fronts are described using models based on a continuum or a discrete representation of the reactive medium. The continuum model can be applied when spatial averaging of the heterogeneous medium is justified, whereas the discrete model does not impose any requirement on the characteristic length of heterogeneity compared to the scale of the front. Using terminology applicable to combustion, the two physical parameters characterizing the reactive system are the ignition temperature $T_{\rm ig}$ and the reaction time t_r, which can be nondimensionlized as $\theta_{\rm ig} = T_{\rm ig}/T_{ad}$ and $\tau_c = t_r/t_d$, which was previously introduced to define the degree of discreteness. Here, T_{ad} is the adiabatic flame temperature of the medium [$T_{ad} = QB/(\rho c_p)$, where Q is the heat release per unit mass of fuel, B is the fuel mass concentration, ρ is the density of the medium, and c_p is the specific heat of the medium]. The thermal diffusivity α, the specific heat c_p, and the density ρ are assumed to be constant.

The position of the front is derived from the temperature field $\theta(\mathbf{x},\tau)$ as the contour of the ignition temperature $\theta_{\rm ig}$ and the temperature field is described by the reaction-diffusion equation with a source term F:

$$\frac{d\theta}{d\tau} = \nabla^2\theta + F. \tag{2}$$

Two closed form, analytic solutions to Eq. (2) are now constructed, one assuming a spatially continuous source term and the other assuming regularly spaced discrete sources.

A. Continuum solution

When the continuum approximation is invoked, the source term F is expressed as a step function in the reaction zone with height $\frac{1}{\tau_c}$ and zero elsewhere. In the steady front-fixed frame, where the ignition front is located at the origin $x = 0$, the reaction zone can be defined as $0 < x < \eta\tau_c$, where the front speed η is given as $\eta = \frac{vl}{\alpha}$. The source term F can be expressed as

$$F = \begin{cases} 0 & \text{if} \quad x < 0 \quad \text{or} \quad x > \eta\tau_c, \\ \frac{1}{\tau_c} & \text{if} \quad 0 \leqslant x \leqslant \eta\tau_c. \end{cases} \tag{3}$$

The front speed η is found by matching the temperature [$\theta(0\pm) = \theta_{\rm ig}$] and the heat flux ($d\theta/dx|_{x=0-} = d\theta/dx|_{x=0+}$) between the diffusion and reaction zones at $x = 0$,

$$\theta_{\rm ig} = \frac{1 - \exp(-\eta^2\tau_c)}{\eta^2\tau_c}. \tag{4}$$

The front speed η calculated from Eq. (4) will be referred to as the *continuum solution* and is plotted as a function of the ignition temperature $\theta_{\rm ig}$ in Fig. 1 (solid curves).

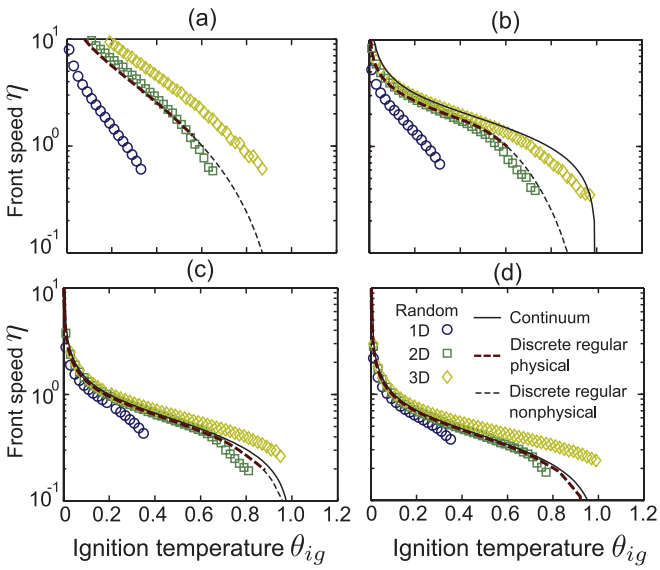

FIG. 1. (Color online) Front speed η as a function of the ignition temperature $\theta_{\rm ig}$ for different reaction times (a) $\tau_c = 0$, (b) $\tau_c = 0.5$, (c) $\tau_c = 5$, and (d) $\tau_c = 10$. The solid line represents the continuum solution; the thick and thin dashed lines are the physical and nonphysical solutions, respectively, calculated using the discrete regular model. The symbols represent the average front speed measured in simulations performed in systems containing randomly distributed sources. The different symbols correspond to a different dimensionality of the system.

B. Discrete regular solution

The discrete solution is obtained for a system of heat sources embedded in an inert, heat conducting medium. The source term F becomes a function of all the individual sources that are reacting. Upon ignition of the ith source at time τ_i, where $i \subseteq N$ and N is the number of reacting sources at time τ_i, the rate of heat release of each source is a temporal δ function when $\tau_c = 0$ and a step function with height $1/\tau_c$ when $\tau_c > 0$. The ignition time τ_i corresponds to the time when the ith source reaches the ignition temperature [i.e., $\theta(\mathbf{x}_i,\tau_i) = \theta_{\rm ig}$]. For a system of N reacting sources at time τ, F is given in the laboratory-fixed frame as

$$F = \begin{cases} \sum_{i=1}^{N} g_i(\mathbf{x})\delta(\tau - \tau_i) & \text{if} \quad \tau_c = 0, \\ \sum_{i=1}^{N} \frac{1}{\tau_c} g_i(\mathbf{x}) H(\tau - \tau_i) H(\tau_c - (\tau - \tau_i)) & \text{if} \quad \tau_c > 0, \end{cases} \tag{5}$$

where H is the Heaviside function. The function $g_i(\mathbf{x})$ reflects the fact that the heat is released from localized sources and is defined by $g_i(\mathbf{x}) = 1$ if $\mathbf{x} = \mathbf{x}_i$ and 0 otherwise, where $\mathbf{x}_i$ is the coordinate vector of the ith reacting source. The position vector $\mathbf{x}_i$ is expressed as a nondimensional length after being normalized with the characteristic intersource spacing l.

This system has the advantage that $\theta(\mathbf{x},\tau)$ can be found by the linear superposition of the solution for each individual reacting source (Green's function), permitting the entire temperature field $\theta(\mathbf{x},\tau)$ to be solved analytically [4,6]. Previous investigations have considered flames in randomized media that are described by Arrhenius kinetics that necessitated simulating the problem via a finite-difference approach, which

limited the simulation to a two-dimensional domain with current computational tools [14]. Using the superposition of Green's functions, the solution to Eqs. (2) and (5) is given as

$$\theta = \begin{cases} \sum_{i=1}^{N} \frac{1}{[4\pi(\Delta\tau_i)]^p} \exp\left(-\frac{|\mathbf{x}-\mathbf{x}_i|^2}{4\Delta\tau_i}\right) \\ \quad \text{if} \quad \tau_c = 0, \\ \sum_{i=1}^{N} \frac{1}{\tau_c} \int_{(\Delta\tau_i-\tau_c)H(\Delta\tau_i-\tau_c)}^{\Delta\tau_i} \frac{1}{(4\pi\zeta)^p} \exp\left(-\frac{|\mathbf{x}-\mathbf{x}_i|^2}{4\zeta}\right) d\zeta \\ \quad \text{if} \quad \tau_c > 0, \end{cases} \tag{6}$$

where the exponent $p = 0.5, 1$, and 1.5 is used in one, two, and three dimensions, respectively, and $\Delta\tau_i = \tau - \tau_i$ is the time elapsed since the ignition of the ith source. The location of the front is derived from the field temperature of the system as the contours corresponding to the ignition temperature θ_{ig}.

Propagating fronts using the discrete model have previously been investigated in systems containing sources distributed in a regular lattice [4,6,11,15]. The methodology and the results are briefly summarized here as a means for comparison with the front properties in systems containing randomly distributed sources. For a one-dimensional system consisting of planar sheets of heat release, the front speed η can be expressed analytically if the sources are placed in a regular array with constant spacing between consecutive sources. In the limit of $N \to \infty$, an implicit solution for the front speed η was obtained for $\tau_c = 0$ by equating Eq. (6) to θ_{ig} and rearranging the terms as $\Delta\tau_i = i/\eta$ and $|\mathbf{x} - \mathbf{x}_i| = i$ [6,15]. These manipulations are equivalent to assuming that the ignition front propagates from source to source with a constant delay time $\Delta\tau = 1/\eta$ between consecutive ignition events. This approach was also used to find η in a regular, three-dimensional array of pointlike sources, and the solution was also extended to $\tau_c > 0$ [4,11]. In fact, a one-dimensional system consisting of evenly spaced planar sheets of heat release is equivalent to a two-dimensional system consisting of a regular array of line sources and a three-dimensional cubic lattice of point sources as $\eta \to 0$ [13]. The front speed is given by the same analytical solution in all three dimensions. The equations used to solve for η as a function of θ_{ig} and τ_c in a regular one-dimensional domain are given in Eq. (7):

$$\theta_{\text{ig}} = \begin{cases} \sum_{i=1}^{\infty} \left(\frac{\eta}{4\pi i}\right)^{0.5} \exp\left(-\frac{i}{4\eta}\right) \\ \quad \text{if} \quad \tau_c = 0, \\ \sum_{i=1}^{\infty} \frac{1}{\tau_c} \int_{(i/\eta-\tau_c)H(i/\eta-\tau_c)}^{i/\eta} \left(\frac{1}{4\pi\zeta}\right)^{0.5} \exp\left(-\frac{i^2}{4\zeta}\right) d\zeta \\ \quad \text{if} \quad \tau_c > 0. \end{cases} \tag{7}$$

This solution will be referred to as the *discrete regular solution*. The relationship between η and θ_{ig} in a regularly spaced system is shown for different values of τ_c in Fig. 1. The thick dashed lines in Fig. 1 correspond to a branch of the solution for η when ignition occurs as $\frac{d\theta}{d\tau} > 0$, while the branch of the solution plotted by the thin dashed lines requires that the temperature decreases upon ignition (i.e., $\frac{d\theta}{d\tau} < 0$). This latter case corresponds to a scenario wherein the temperature at the source first passes through the ignition temperature without igniting, then does ignite upon encountering the ignition temperature for a second time as temperature decreases. The unphysical ignition condition is indicative of an inherent propagation limit in regular arrays [11,13], as described further below.

The discrete and the continuum models are in agreement when $\tau_c \gg 1$, as shown in Figs. 1(c) and 1(d). For $\tau_c < 1$, the continuum model significantly overpredicts η due to neglecting the diffusion time required for the front to advance between neighboring sources, as shown in Fig. 1(b). In fact, for $\tau_c = 0$ [Fig. 1(a)], the continuum solution predicts an infinite front speed while the discrete regular model yields a finite value. As opposed to the continuum theory, the discrete model accounts for the diffusion time between sources during which no new ignition event occurs, which acts as a mechanism limiting the front speed.

The difference between the discrete and continuous regimes is also reflected in the propagation limit. The continuum model implies that if the heat released by all of the sources can elevate the average temperature of the system to T_{ig}, then the front can propagate. This condition defines a *thermodynamic limit* to flame propagation, denoted by $\theta_{\text{ig,th}} = 1$, which is independent of τ_c. However, in a system containing regularly distributed sources, the effect of localizing the heat release introduces an inherent limitation to propagation related to the fact that physically, ignition must occur as temperature increases. Failure to comply with this condition renders the solution unphysical, as illustrated in Fig. 1 by the unphysical branch of η represented by the thin dashed line. This condition can be expressed as a critical ignition temperature $\theta_{\text{ig,cr}}$ associated with the condition $\frac{d\theta}{d\tau} = 0$ at ignition. For $\tau_c = 0$, we find $\theta_{\text{ig,cr}} \approx 0.568$ and this value is closely associated with the propagation limit. As the ignition temperature of the sources approaches the critical condition, the dynamics of the wave propagation become increasingly complex, due to the extreme sensitivity of the ignition time to the nearly flat temperature profile prior to ignition. Indeed, if the transient dynamics of the system are solved for τ_i [rather than assuming a fixed time delay between ignitions as in Eqs. (6) and (7)], the delay time between successive ignitions undergoes a series of bifurcations beginning at $\theta_{\text{ig,bif}} \approx 0.512$ and becomes fully chaotic as θ_{ig} is increased [6,11,15], leading to a propagation limit at $\theta_{\text{ig,lim}} \approx 0.534$. This result highlights one of the unique aspects of discrete reactive fronts that differentiates it from the conventional continuum theory: a propagation limit in the absence of losses that is encountered far from the thermodynamic limit.

This propagation limit is attributed to the fact that, in the discrete regime, heat release remains spatially concentrated around sources, giving rise to an internal loss mechanism, permitting heat to diffuse backward rather than only forward in the direction of the propagation of the front. As a result, a limit to propagation is encountered in regularly spaced, discrete systems at approximately half the ignition temperature (or, alternatively, twice the heat release or twice the fuel concentration) as predicted by the thermodynamic limit.

IV. DISCRETE RANDOM SOLUTION

The results discussed so far are limited to a regular distribution of sources. We will now consider sources distributed randomly in space in one-, two-, and three-dimensional systems. A random number generator [16] was used to generate clouds of up to 20 000 sources randomly positioned in space. After a subset of the sources were prescribed to ignite in

order to initiate a propagating front at time $\tau = 0$, Eq. (6) was used to calculate the temperature field and find the time at which unreacted sources reached the ignition temperature θ_{ig}. The source with shortest ignition time τ_i was identified as the next reacting source and was then added to the pool of reacted sources used to compute the ignition time of the next unreacted source. The solution was then advanced until all the sources in the domain had been ignited or no additional unreacted source reached the ignition temperature θ_{ig} and the front quenched. This solution will be referred to as the *discrete random solution*.

In all simulations, the concentration of sources was set to unity in the domain. In one, two, and three dimensions, this corresponded to a single source per unit length, area, and volume, respectively. The number density of sources was the same for discrete regular solution presented in Sec. III B. In one dimension, computations were performed in domains up to a length $l_x = 2 \times 10^4$. Two-dimensional simulations were limited to a square domain and the domain length l_x was varied from 50 to 90. In three dimensions, the geometry was constrained to a cube with a side length l_x that was varied from 20 to 25. In the latter case, the domain size was limited by computational capacity, which was rapidly reached in view of the fact that the number of candidates that must be considered as the next activated source increases rapidly as we move from one- to two- to three-dimensional systems. The next reacting source candidate in one-dimension is simply the next unreacted source neighboring the last reacted source. In multidimensional systems, the next reacting source is only found after the ignition times of all unreacted sources in the near vicinity of the front have been calculated.

In two and three dimensions, periodic boundary conditions were imposed to the sides of the domain to eliminate the heat losses and to isolate effects arising from using a finite-sized domain. The upstream and downstream boundaries along the x axis (i.e., the axis of propagation) remained free. Periodic boundary conditions were implemented by introducing images of a reacting source upon its ignition outside the boundaries of the domain. In two dimensions, if a source reacted at coordinates (x_i, y_i), then multiple release sites were simultaneously positioned outside the domain, at location $(x_i, y_i \pm m l_x)$. In three dimensions, images were placed in the y and z directions, but also in quadrants located in the diagonal directions of the domain. The coordinates of the images are given by $(x_i, y_i \pm m l_x, z_i \pm n l_x)$ where the index variables $\{m,n\} \subset \mathbb{N}$ and represent the image number, which in principle should tend to infinity to simulate an infinitely large domain. In practice, it was found that considering images with $\{m,n\} = \{1,2\}$ was sufficient; considering additional mirror images did not influence the front.

A constant-volume explosion approach was used to initiate the front. In other words, all the sources in a portion of the domain were forced to ignite at time $\tau = 0$. Figure 2 illustrates the appearance of the system at initiation in one-, two-, and three-dimensional systems. This initiating region contained a variable number of sources determined by the random source distribution and the initiation length l_i (the distance from $x = 0$ to the plane separating the initiating domain from the freely propagating domain). The amount of heat released by the initiating sources was also artificially increased to ensure the formation of a propagating front. The heat released by the initiating sources was quantified by the overdrive parameter Ω, defined as the ratio between the heat released by the initiating sources and the sources in the propagating domain. The overdrive parameter is necessary for the constant-volume explosion approach because a front can be initiated in the freely propagating domain only if the overdrive is larger than the ignition temperature [17]. Ensuing that the propagation limits and front speeds measured in the simulations were a fundamental property of the medium, and not the result of a failure to initiate the front or influenced (i.e., overdriven) by the parameters of initiation (Ω or l_i), comprised a major portion of the effort in this study.

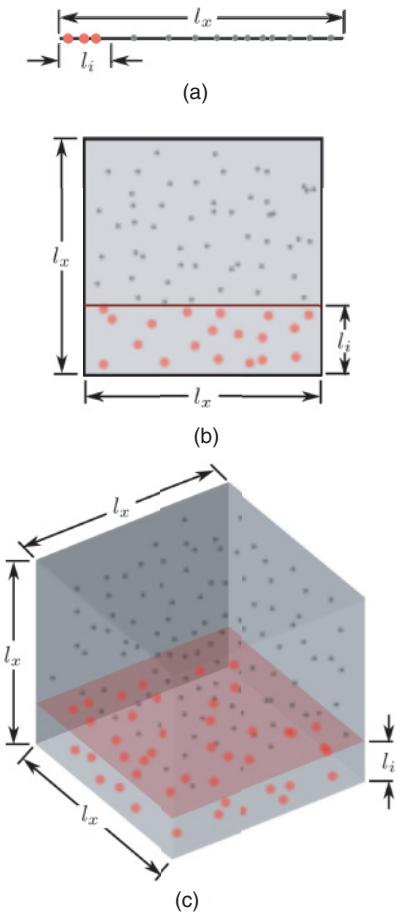

FIG. 2. (Color online) Schematic diagrams of (a) one-, (b) two-, and (c) three-dimensional systems with randomly distributed sources upon ignition. The large dots represent overdriven sources force-ignited and the sources inside the freely propagating domain are shown as small dots.

The appearance of a propagating front in one-, two-, and three-dimensional systems with sources randomly distributed for $\tau_c = 0$ is shown in Fig. 3. In Fig. 3(a), the one-dimensional temperature field is described by the solid line. In Fig. 3(b), the two-dimensional ignition temperature contour is shown as the solid line and the temperature field is represented by shading. In Fig. 3(c), the temperature field in the three-dimensional simulation is only visible on three sides of the domain and the front marking the ignition temperature is represented by the surface propagating upward.

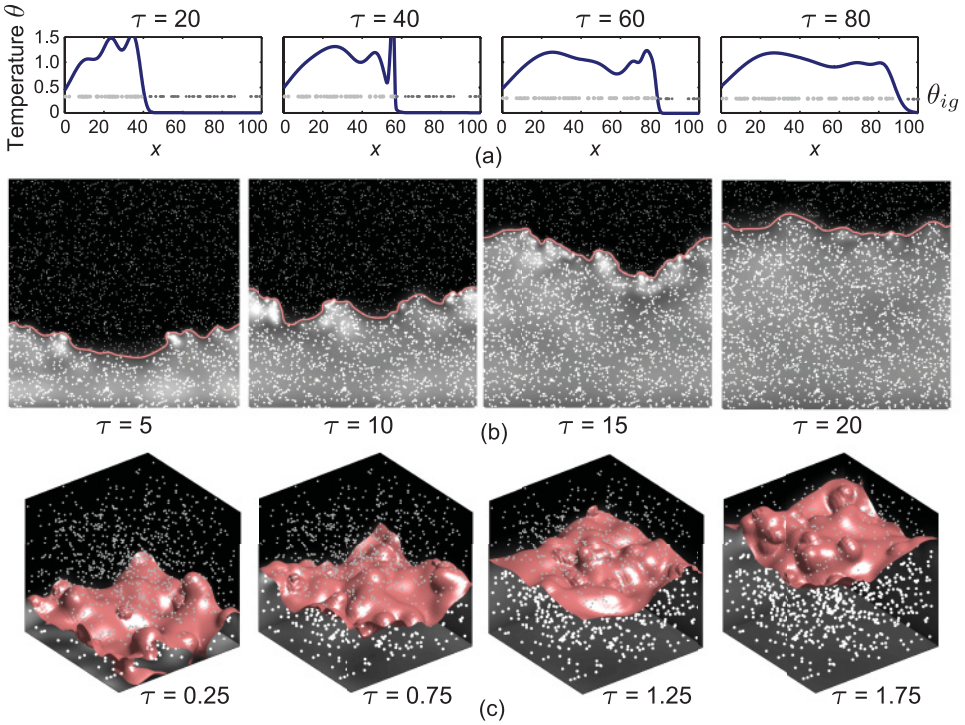

FIG. 3. (Color online) Simulations of reaction fronts propagating in (a) one-, (b) two-, and (c) three-dimensional random systems in the discrete regime ($\tau_c = 0$). The sources are shown in light gray if reacted and dark gray if unreacted. In (a) the front is propagating from left to right and in (b) and (c) the front is propagating upward. In (a), the y coordinates of the sources indicate the ignition temperature $\theta_{ig} = 0.3$. In (b) and (c), the contour line and the surface represent the isotherm of the ignition temperature $\theta_{ig} = 0.5$.

V. RESULTS

In this work, the influence of randomly distributed sources on the propagation of the front is studied by determining two quantities: the propagation limit and the front speed. These quantities are expressed as probabilistic values and reflect multiple simulations performed using different randomized distributions with the same global parameters of source density, ignition temperature θ_{ig}, and reaction time τ_c. The results obtained in random distributions of sources are compared with the continuum theory (Sec. III A) and the discrete regular solution (Sec. III B).

A. Propagation limits in randomized systems

The propagation limit is defined by the ignition temperature at quenching $\theta_{ig,qc}$ marking a change in the outcome of a simulation: whether the front successfully propagates from the initiation end to the far end of the domain or whether the front quenches before reaching the end of the domain. In media characterized by $\theta_{ig} \ll \theta_{ig,qc}$, the front always propagated from end-to-end. If $\theta_{ig} \gg \theta_{ig,qc}$, the front promptly quenches in all simulations. Near the value of $\theta_{ig,qc}$, both successful propagation and quenching were observed. This feature emphasizes the necessity to consider the outcome of any particular simulation with randomly spaced sources as being probabilistic. To define a numerical value for $\theta_{ig,qc}$, multiple simulations using different spatial distributions of sources were performed for a range of ignition temperatures θ_{ig}, while keeping the reaction time τ_c fixed. For each value of the ignition temperature θ_{ig}, the propagation probability $P(\theta_{ig})$ was calculated by normalizing the number of simulations where the front propagated successfully end-to-end, N_s, with the total number of simulations performed N_t. The ignition temperature at quenching $\theta_{ig,qc}$ was obtained by fitting the propagation probability P to the ignition temperature θ_{ig} using the integral of the Gaussian [18]:

$$P(\theta_{ig}) = \frac{1}{2}\left[1 - \mathrm{erf}\left(\frac{\theta_{ig} - \theta_{ig,qc}}{\sigma_{qc}\sqrt{2}}\right)\right], \tag{8}$$

where σ_{qc} quantifies the steepness of the transition from a propagating to a quenching outcome as the ignition temperature θ_{ig} increases. In other words, in randomized systems, the ignition temperature at quenching $\theta_{ig,qc}$ is defined by the condition $P(\theta_{ig,qc}) = 0.5$.

Figure 4 shows the propagation probability P in random one-dimensional systems in which the domain length l_x is

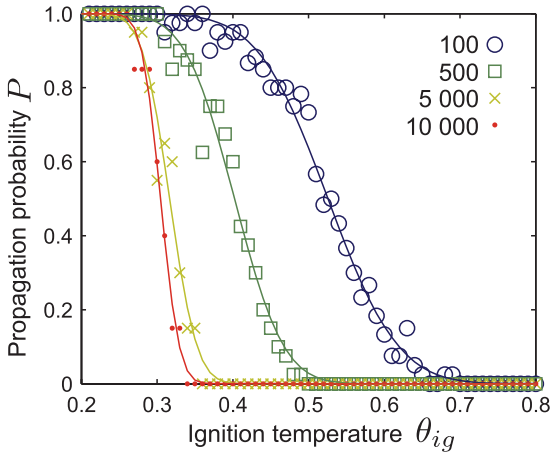

FIG. 4. (Color online) Propagation probability P in a one-dimensional random system as a function of the ignition temperature. The different symbols represent different domain lengths l_x. The initiation length $l_i = 5$, the overdrive $\Omega = 10$, and a reaction time $\tau_c = 0$ remained unchanged. For each domain length l_x, the solid lines represent curve fits using Eq. (8).

increased from 100 to 10 000. The propagation probability P was calculated from a set of 20 simulations for each value of the ignition temperature $\theta_{\rm ig}$ and each simulation was computed in a unique random spatial distribution of the sources. The curves fitted to the propagation probability P for each domain length l_x were obtained from Eq. (8). The results in Fig. 4 are obtained for a one-dimensional system, but a qualitatively similar behavior is observed in two- and three-dimensional systems as well.

1. Propagation limit in one dimension

Simulations were performed with one-dimensional arrays of randomly positioned sources of heat release. The ignition temperature at which quenching occurred $\theta_{\rm ig,qc}$ was determined for a fixed reaction time τ_c and for different domain lengths l_x and initiation parameters. Figure 5(a) shows the ignition temperature at quenching $\theta_{\rm ig,qc}$ for $\tau_c = 0$ as a function of the overdrive Ω and for varying domain lengths l_x, while keeping the initiation length constant $l_i = 5$. In Fig. 5(b), $\theta_{\rm ig,qc}$ is plotted against the initiation length l_i for an overdrive $\Omega = 10$.

For lower values of the overdrive Ω or the initiation length l_i, the initiating region was unable to reliably initiate a propagating front, resulting in a value of $\theta_{\rm ig,qc}$ being artificially low. For larger values of Ω or l_i, the front can become overdriven in smaller-sized domains (e.g., $l_x = \{100,200\}$) by the large amount of heat diffusing forward from the initiating region, resulting in an artificially increased value of $\theta_{\rm ig,qc}$. For example, as the initiating region occupies a larger portion of the domain, the front is obviously more likely to successfully propagate across the remainder of the domain. In between these two cases, in most simulations a "plateau" value of $\theta_{\rm ig,qc}$ could be identified that is independent of the overdrive parameter or the length of the initiating region. Note that in the smallest domain considered ($l_x = 100$), no such plateau could be identified, due to a continuous transition from an ineffective initiation to an overdriven propagation.

In one-dimensional simulations, the region where $\theta_{\rm ig,qc}$ displays a plateau (i.e., the value where $\theta_{\rm ig,qc}$ is independent of the initiation parameters) was found to always be dependent upon the domain length l_x. As shown in Figs. 5(a) and 5(b), as the domain size l_x increases, the plateau value of $\theta_{\rm ig,qc}$ continues to decrease. This result reflects the fact that, in one dimension, increasing the domain size increases the likelihood that the random placement of sources will eventually result in a gap of sufficient size that the front is not able to successfully traverse. In this work, the propagation limit $\theta_{\rm ig,lim}$ is defined as the plateau value of $\theta_{\rm ig,qc}$ with the condition that the plateau is independent of the domain size and the initiating conditions. Thus, for a one-dimensional randomized system, a fundamental propagation limit cannot be defined. It is also interesting to note that, compared to a one-dimensional system with regularly spaced sources, randomness of the sources appears to be detrimental to the propagation of the front. In all simulations where a value of $\theta_{\rm ig,qc}$ could be found, the value was less than 0.5, while in a one-dimensional system with regularly spaced sources, the front can successfully propagate up to a value of $\theta_{\rm ig,qc} = 0.534$ [6,11,13,15].

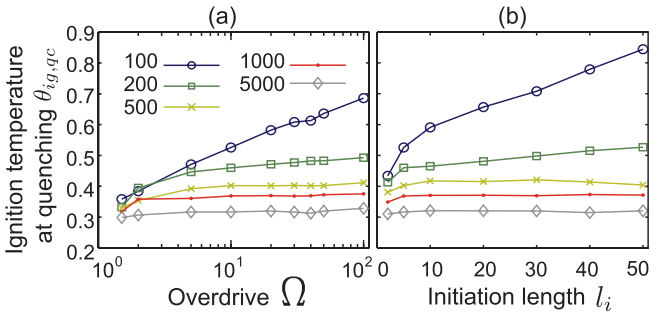

FIG. 5. (Color online) Ignition temperature at quenching $\theta_{\rm ig,qc}$ as a function of (a) the overdrive Ω and (b) the initiation length l_i in a one-dimensional system. The different symbols represent different domain lengths.

2. Propagation limit in two and three dimensions

Our previous attempt [13] to determine the propagation limit $\theta_{\rm ig,lim}$ in two dimensions considered domains of increasing width, but in which the domain length and the initiating conditions were kept constant. As the domain widened, the front was able to propagate end-to-end at increasingly larger values of the ignition temperature $\theta_{\rm ig}$ until the width increased to approximately 80 units and the ignition temperature at quenching began to plateau at $\theta_{\rm ig,qc} \approx 0.64$. In the present work, the propagation of the front is studied in two-dimensional geometries with varying size and fixed aspect ratio equal to unity (i.e., square domains) and the initiation conditions are varied to determine the propagation limit $\theta_{\rm ig,lim}$.

Results of two-dimensional simulations with up to 8100 randomly distributed sources are shown in Fig. 6 for the case $\tau_c = 0$. Following the same analysis performed for one-dimensional systems, the ignition temperature at quenching $\theta_{\rm ig,qc}$ was determined for a given set of parameters ($\theta_{\rm ig}$, l_x, l_i, Ω). Smaller values of the overdrive and the initial length resulted in a failure to initiate the front, as reflected in lower values of $\theta_{\rm ig,qc}$. Larger values of l_i and Ω overdrove the front, resulting in greater values of $\theta_{ig,qc}$. Between these two extremes, a plateau value of $\theta_{ig,qc}$ was identified, although this plateau is not as self-evident in two dimensions as in one

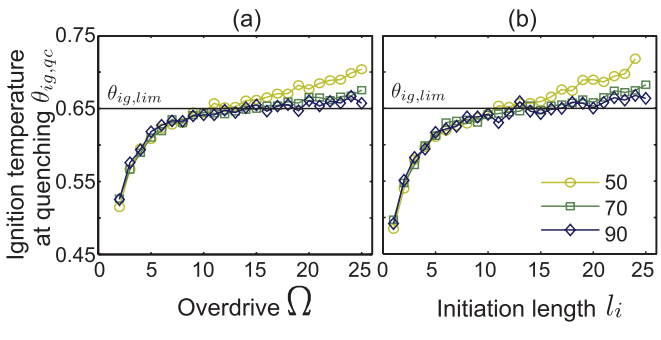

FIG. 6. (Color online) Ignition temperature at quenching $\theta_{\rm ig,qc}$ as a function of (a) the overdrive Ω (with constant initiation length $l_i = 1$) and (b) the initiation length l_i (with constant overdrive $\Omega = 1.5$) in two-dimensional random systems. The reaction time is fixed $\tau_c = 0$ and each symbol represents a different domain length l_x. The horizontal line indicates the value of the propagation limit found, $\theta_{\rm ig,lim} \approx 0.65$.

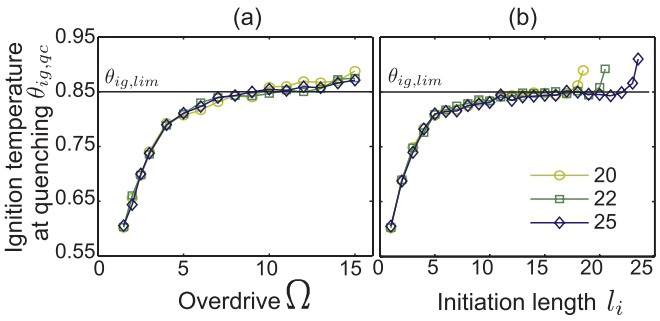

FIG. 7. (Color online) Ignition temperature at quenching $\theta_{\mathrm{ig,qc}}$ as a function of (a) the overdrive Ω (with constant initiation length $l_i = 1$) and (b) the initiation length l_i (with constant overdrive $\Omega = 1.5$) in three-dimensional random systems. The reaction time is $\tau_c = 0$ and each symbol represents a different domain length. The horizontal line indicates the value of the propagation limit found, $\theta_{\mathrm{ig,lim}} \approx 0.85$.

dimension. We attribute this result to smaller domain sizes that were used for two-dimensional calculations. The plateau appears more as an inflection point for the curves in Fig. 6.

Figures 6(a) and 6(b) show that the size of the domain l_x does not affect $\theta_{\mathrm{ig,qc}}$ in two-dimensions when the domain length l_x exceeds 50. The effect of lengthening the domain, and thus increasing the quenching probability, appears to be equally balanced by increasing the domain width, which effectively introduces additional propagation paths and increases the probability of successful propagation. As opposed to one-dimensional systems, a propagation limit in two dimensions can be expressed independently of the domain size if the domain is sufficiently large. This limit for the case of $\tau_c = 0$ is found to be $\theta_{\mathrm{ig,lim}} \approx 0.650 \pm 0.005$, and this value is believed to be the fundamental limit to propagation in two-dimensional systems with random, discrete sources.

Similar simulations were performed in three dimensions with up to 15 625 sources. In three dimensions, due to computation limitations, the largest domain considered had a size of $l_x = 25$. As in two dimensions, we first considered the effect of varying the overdrive Ω, while fixing the initiation length $l_i = 1$ [Fig. 7(a)]. For smaller domains ($l_x = 20$), the front directly transitions from an underdriven to an overdriven initiation and a plateau value of $\theta_{\mathrm{ig,lim}} \approx 0.850 \pm 0.003$ only becomes apparent for larger domains $l_x = \{22,25\}$ for $10 \leqslant \Omega \leqslant 13$, as shown in Fig. 7(a). When $\Omega = 1.5$ [Fig. 7(b)], increasing the initiation length does permit a plateau to be identified at approximately the same value ($\theta_{\mathrm{ig,lim}} \approx 0.850$), giving confidence that this value is independent of the initiation parameters. A summary of the values of the fundamental propagation limit found in two- and three-dimensional systems is given in Table I.

TABLE I. Summary of the propagation limits in one-, two-, and three-dimensional systems according to the continuum solution, and the discrete regular and random solutions for $\tau_c = 0$.

Model	1D	2D	3D
Continuum $\theta_{\mathrm{ig,th}}$	1.00	1.00	1.00
Discrete regular $\theta_{\mathrm{ig,lim}}$	0.534	0.534	0.534
Discrete random $\theta_{\mathrm{ig,lim}}$	n/a	0.650 ± 0.005	0.853 ± 0.005

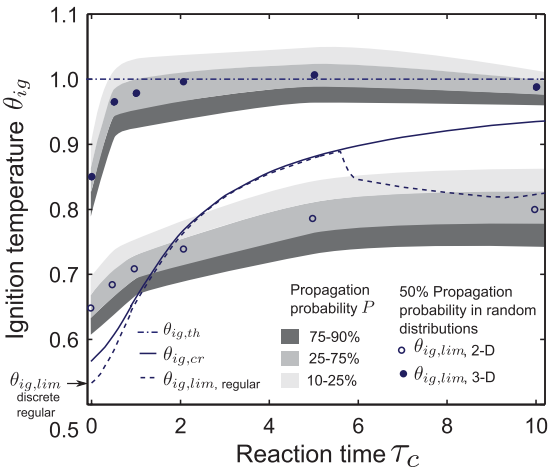

FIG. 8. (Color online) Propagation limit $\theta_{\mathrm{ig,lim}}$ as function of the reaction time τ_c in two- and three-dimensional systems with randomly positioned sources (symbols). The gray shading bands correspond to propagation probability intervals. The solid line is the critical ignition temperature $\theta_{\mathrm{ig,cr}}$, the dashed line is the propagation limit $\theta_{\mathrm{ig,lim}}$ for a regular array of sources, and the dash-dotted line is the thermodynamic limit $\theta_{\mathrm{ig,th}}$.

The effect of increasing the reaction time τ_c, which also plays the role of the discreteness parameter, on the fundamental propagation limit was studied to examine whether the behavior would revert to continuum-like behavior for sufficiently large τ_c. The domain size l_x was fixed to 80 in two dimensions and 22 in three dimensions, while the initiation conditions were changed by varying the overdrive Ω and fixing the initiation length $l_i = 1$ in order to determine the plateau value of $\theta_{\mathrm{ig,qc}}$. The propagation limits $\theta_{\mathrm{ig,lim}}$ found in two and three dimensions are shown in Fig. 8 and compared to the propagation limit obtained in a regular distribution $\theta_{\mathrm{ig,lim}}$ [13]. The shaded bands quantifying propagation probability intervals were obtained from the steepness parameter σ_{qc}, which represents the one-standard-deviation interval for $\theta_{\mathrm{ig,qc}}$ [i.e., $P(\theta_{\mathrm{ig,qc}} \pm \sigma_{\mathrm{qc}}) = \frac{1}{2}(1 \pm \mathrm{erf}\frac{1}{\sqrt{2}})$]. The critical ignition temperature $\theta_{\mathrm{ig,cr}}$, which quantifies the condition $d\theta/d\tau = 0$ at ignition and is solved for using Eq. (7), is also plotted as a function of τ_c in Fig. 8. The relationship between the critical ignition temperature $\theta_{\mathrm{ig,cr}}$ and τ_c illustrates the convergence of the critical ignition temperature $\theta_{\mathrm{ig,cr}}$ associated with Eq. (7) toward the thermodynamic limit $\theta_{\mathrm{ig,th}}$ as τ_c increases [13].

The results obtained in one-dimensional, random systems are not shown because the propagation limit $\theta_{\mathrm{ig,lim}}$ could not be defined. The propagation limit $\theta_{\mathrm{ig,lim}}$ in regular arrays (the dashed curve in Fig. 8) is the same for all dimensions and exhibits a sawtooth-shaped curve due to alternating changes of the quenching mechanism between prompt quenching of the front and the growth of oscillations of the front speed [13].

In three dimensions, randomizing the position of the sources is beneficial to the propagation of the front. The effect of randomizing the sources effectively eliminates the dynamics associated with quenching in systems containing sources regularly distributed for larger values of τ_c (i.e., the sawtooth curve in Fig. 8). The propagation limit $\theta_{\mathrm{ig,lim}}$ in three-dimensional random systems appears to converge rapidly

toward the thermodynamic limit $\theta_{ig,th}$ as the discreteness parameter τ_c is increased. In two dimensions, the propagation limit $\theta_{ig,lim}$ increases with τ_c, but the propagation limit in a system with regularly spaced sources then exceeds the value found for two-dimensional random systems when $\tau_c > 2$. The propagation limit $\theta_{ig,lim}$ in two dimensions asymptotes toward a value approaching 0.80 as τ_c increases. The fact that the front remains limited to propagate within a two-dimensional domain prevents the propagation limit $\theta_{ig,lim}$ from reaching the thermodynamic limit $\theta_{ig,th} = 1$.

B. Front speed

In addition to the propagation limits, the average front speed η can also be used to quantify the behavior of the front under conditions far from quenching. In one dimension, the location of the front x_f along the direction of propagation can be defined clearly, whereas two- and three-dimensional fronts are represented by curvilinear lines and surfaces. The fact that the position of the front is no longer described by a single quantity requires a procedure to track the overall propagation. Three different techniques have been considered to quantify the average front speed in multidimensional systems. The front speed was calculated by (1) fitting a line through the $x_p(\tau)$-τ diagram, where x_p is the x location of the source ignited farthest away from the initiation end of the domain at time τ, (2) fitting a line through the x_i-τ_i diagram, where x_i represents the x location of the ith source ignited at time τ_i, and (3) collapsing the temperature field in two and three dimensions onto a one-dimensional system by averaging the temperature at a given x location along a line in the y direction or a y-z plane in two or three dimensions, respectively; the position of the front is obtained by tracking the location where the averaged temperature on the x axis equals the ignition temperature. The three methods yielded the same average front speed provided a sufficiently large domain was used. The results discussed below have been computed using the second method (using a line fit through the x_i-τ_i data sets), but are effectively independent of the method used to calculate the front speed. Examples of the x_i-τ_i diagrams for one-, two-, and three-dimensional systems are plotted in Fig. 9. The x_i-τ_i data plotted in Fig. 9(b) for a two-dimensional random simulation shows evidence of striated bands that propagate much faster than the global average front speed. Analysis of the simulations revealed that these bands are caused by a rapid sequence of ignition sweeping through clusters that naturally arise when sources are randomly positioned. These striations also occur in three-dimensional random systems, but these bands are more difficult to identify in Fig. 9(c) due to their projection onto a one-dimensional representation.

The front speed was measured using the average of ten simulations using the same ignition temperature θ_{ig} and the reaction time τ_c, but different randomized distributions of the sources. From the set of simulations performed, the front speed is only reported on Fig. 1 if the propagation probability $P \geqslant 0.5$. The average front speeds η for one-, two-, and three- dimensional systems of randomly spaced sources are compared to the front speed in a regular source distribution as well as the continuum solution in Fig. 1. The corresponding

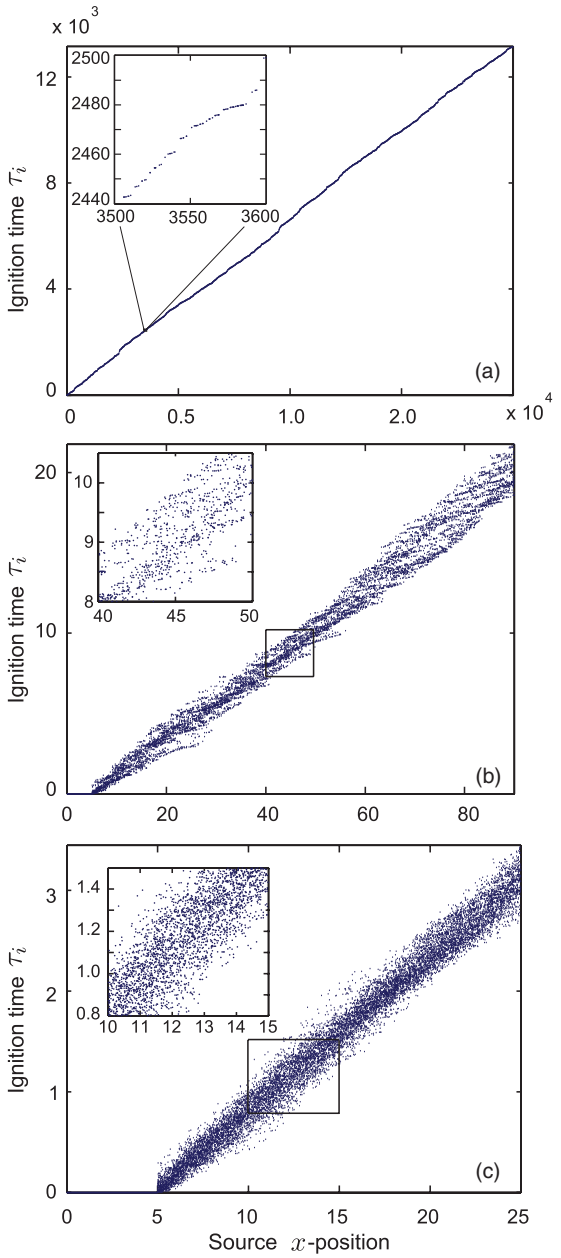

FIG. 9. (Color online) Typical space-time diagrams of ignition events in (a) 1D ($l_x = 2 \times 10^4$), (b) 2D ($l_x = 90$), and (c) 3D ($l_x = 25$). The reaction time is $\tau_c = 0$ and the ignition temperature is $\theta_{ig} = 0.3$.

standard deviations are negligible. In one dimension, the front speed η is effectively independent of the initiation conditions due to fact that the domain length considered (i.e., $l_x = 2 \times 10^4$) is sufficiently long to remove any influence on the front speed due to initiation. In two and three dimensions, the initiation conditions do not affect the average front speed η provided that the line fit was performed after an initial transient period in which the front first established itself.

Note that the solution plotted in Fig. 1 for regularly distributed sources is calculated analytically from Eqs. (6) and (7) that imposed a fixed periodicity to the sequence of initiation of the sources, and is not obtained via simulations in which the source is triggered as it reaches the ignition temperature

as determined by the evolving solution. Thus, the discrete regular solution does not exhibit the instabilities associated with ignition and can be plotted up to the thermodynamic limit $\theta_{ig,th} = 1$. As discussed in Sec. III B, this analytic solution exhibits an unphysical property for values of $\theta_{ig} > \theta_{ig,cr}$ where ignition occurs upon a decreasing temperature, rather than upon first encountering the ignition temperature; this unphysical branch is plotted as a thin dashed line in Fig. 1.

The average front speed η significantly deviates from the discrete regular model in one and three dimensions for $\tau_c < 1$, but approaches the solution given by Eq. (6) as τ_c increases. However, the front speed η in three-dimensional, random systems never reaches 0 as θ_{ig} tends to 1, even for larger values of τ_c. In two dimensions, the front speed measured for random systems is approximately the same as the discrete regular solution.

In random systems, the average front speeds are always greater in three dimensions than in one and two dimensions, and the two-dimensional fronts always propagate faster than in one dimension. This feature is particularly evident for $\tau_c = 0$, where the dimensionality of the system has the strongest influence on the front speed. This result may indicate that the front is dominated by local interactions within clusters that are inherent in randomly positioned sources when $\tau_c \ll 1$. When $\tau_c \to \infty$, the discreteness and dimensionality of the system do not significantly affect the front speed.

VI. DISCUSSION AND CONCLUDING REMARKS

Reaction-diffusion fronts propagating in a system consisting of pointlike sources embedded in an inert medium can be profoundly influenced by the discrete nature of the sources. In order to determine the significance of the effect of discreteness or whether a space-averaging procedure is appropriate, the discreteness parameter τ_c, which is the ratio of the reaction time t_r to the characteristic diffusion time between sources t_d, should be examined. When $\tau_c \gg 1$, the scale of the heterogeneity is sufficiently small in comparison to the effective reaction zone thickness that assuming the source term to be spatially uniform in the reaction zone is an appropriate approximation. For $\tau_c < 1$, the propagation of the front is dominated by the effects of discreteness. Two consequences of discreteness investigated in this paper were (1) a propagation limit that occurs due to the discrete nature of the front that cannot be predicted from purely thermodynamic considerations and (2) a front speed that is considerably different than that predicted by a continuum model that neglects the diffusion time between consecutive ignition events.

A strong influence of dimensionality of the system is seen on both the propagation limit and the propagation speed for systems with randomly positioned sources. In one-dimensional systems with randomly position sources, it is not possible to define a fundamental propagation limit independent of the domain size, since as the domain is made larger, the likelihood of encountering a gap that will result in failure of the front always increases. This condition may be associated with the front being dimensionally constrained such that a source can only sequentially influence its immediate neighbor. In this sense, the one-dimensional system considered here is pathological, similar to the well-known pathological behavior (i.e., anomalous heat conduction and diffusion, a lack of thermalization, etc.) in one-dimensional lattices and fluids. In two- and three-dimensional systems, however, it is possible to define a fundamental limit to propagation that appears to be independent of the domain size. This limit is found to be different than that predicted by the continuum solution for the equivalent homogeneous system and also different than the limit found in a system of regularly spaced discrete sources. Due to the statistical nature of phenomena resulting from systems with randomly positioned sources, the propagation limit can only be defined probabilistically. In this work, the propagation limit is defined as the nondimensional ignition temperature θ_{ig} for a given nondimensional reaction time τ_c that results in a 50% probability that a front will propagate across a domain. Demonstrating that this limit is independent of domain size and the method used to initiate the reactive front involved performing a very large number of simulations in which these parameters were varied systematically.

In two-dimensional systems with randomly positioned sources, the propagation limit is encountered at $\theta_{ig} \approx 0.65$ (in comparison to the dimension-independent value of $\theta_{ig} = 0.534$ for regularly spaced systems) in the limit of instantaneous reaction time $\tau_c = 0$. The ability of a front in systems with randomized sources to propagate under conditions that would otherwise demand unphysical ignitions in a regular system has been observed in prior work [12]. As τ_c is increased, the two-dimensional random system does not revert back to the thermodynamic limit $\theta_{ig,th} = 1$, suggesting that the front (similar to the discrete regular solution) is still influenced by front dynamics that result in quenching. For three-dimensional systems with randomly positioned sources, the propagation limit at $\tau_c = 0$ is encountered at $\theta_{ig} \approx 0.85$, and quickly increases to a value close to the thermodynamic limit $\theta_{ig,th} = 1$ as the value of τ_c is increased to the order of unity. The fact that the statistically defined propagation limit has a value of $\theta_{ig,lim} \approx 1$ means that there is a finite probability that the front may propagate in a system with $\theta_{ig} > \theta_{ig,th}$. This result is visible in Fig. 8 by the shaded band exceeding a value of $\theta_{ig} = 1$ for three-dimensional random systems. As τ_c is increased further (i.e., $\tau_c \gg 1$), the transition between regions of quenching and successful propagation becomes sharper (as indicated by a decreasing value of σ_{qc}), and the solution band narrows to converge to the thermodynamic limit which, being continuum based, does not exhibit a probabilistic nature.

A similar strong influence of system dimensionality is seen when examining the front speed. A front in a three-dimensional system of randomly positioned sources propagates faster than the corresponding two-dimensional system, which in turn is always faster than a one-dimensional system when the propagation occurs in the discrete regime ($\tau_c < 1$), while in a system of regularly space sources, the propagation speed is independent of the system dimension. As the value of the dimensionless reaction time τ_c is increased, the solutions for front speed in different dimensions collapse together with the discrete regular and continuum-based solutions over most of the values of ignition temperature, as seen in Fig. 1. However, for large values of θ_{ig} near the thermodynamic limit, the three-dimensional random system can exhibit propagation speeds that exceed even the continuum-based solution as seen in Figs. 1(c) and 1(d), and this effect persists for large values of $\tau_c \approx 10$. The fact that

a discrete system in which heat must diffuse from source to source can exceed the propagation speed of an equivalent homogenized system is strong evidence that a three-dimensional system is able to exploit local fluctuations in concentration that are inherent to randomly generated arrays of sources.

The results obtained between different dimensions of discrete random systems and those in comparison to the discrete regular and the equivalent continuum systems share a number of high-level features that had previously been observed in fronts propagating through a Belousov-Zhabotinsky (BZ) medium containing spatially excited random fluctuations [19]. Although the BZ reaction is expressed in a disordered continuum, rather than an array of pointlike sources considered in the present paper, the front speed was larger in a two-dimensional compared to a one-dimensional spatially randomized system. This feature, similar to the results obtained with the present discrete random model, highlights an enhanced propagation due to the roughening of the front resulting from the randomness of the medium. In addition, Sendiña-Nadal *et al*. observed that in a two-dimensional system, the propagation velocity in a disordered continuum exceeds the velocity in an equivalent homogenized system, a result that was also obtained in the present study in a three-dimensional system.

The phenomenon studied here has some characteristics of directed percolation [20,21], which also exhibits a strong dependence on the dimensionality of a randomized medium and which also cannot typically be observed in one-dimensional systems. Similar to percolation, critical values of system parameters (e.g., source densities) can only be found by computational simulations and cannot be derived from a mean-field theory approach. We do not believe, however, that the phenomenon described in this paper can be treated using traditional percolation theory, since percolation theory usually limits interactions over a finite range (typically, with nearest neighbors only), while in reaction-diffusion systems governed by the diffusion equation, the domain of influence of a given source is, in principle, infinite and influences all subsequent time.

Evidence of experimental realization of this discrete regime of propagation has been recently reported in an experimental system consisting of iron particles in suspension in a gaseous oxidizer [12]. Substituting the nitrogen in air for xenon permitted the thermal diffusivity of the gaseous medium to be sufficiently lowered, resulting in the flame propagating through the reactive mixture being in the discrete regime. Substituting the nitrogen with helium (with high thermal conductivity) enabled the continuum regime to be realized. The experimental measurements of the flame speed in xenon-balanced mixtures exhibited a weaker dependence of the flame speed on the particle burning time, indicative of the discrete regime, compared to results obtained with helium-balanced mixtures, which were in better agreement with continuum theory predictions. Further investigations of other reactive systems that may exhibit discrete behavior are underway.

ACKNOWLEDGMENTS

This work was supported by the Canadian Space Agency under Contract No. CSA-9F007052073. This research has been enabled by the use of computing resources provided by WestGrid, Sharcnet, RQCHP, CLUMEQ, and Compute/Calcul Canada.

[1] J. Xin, SIAM Rev. **42**, 161 (2000).
[2] A. Mukasyan and A. Rogachev, Prog. Energy Combust. **34**, 377 (2008).
[3] V. Mendez and J. E. Llebot, Phys. Rev. E **56**, 6557 (1997).
[4] S. Goroshin, J. H. S. Lee, and Y. Shoshin, Symp. (Int.) Combust. **27**, 743 (1998).
[5] A. Atri, J. Amundson, D. Clapham, and J. Sneyd, Biophys. J. **65**, 1727 (1993).
[6] J. Keizer, G. D. Smith, S. Ponce-Dawson, and J. E. Pearson, Biophys. J. **75**, 595 (1996).
[7] S. P. Dawson, J. Keizer, and J. E. Pearson, Natl. Acad. Sci. U.S.A. **96**, 6060 (1999).
[8] A. G. Merzhanov and E. N. Rumanov, Rev. Mod. Phys. **71**, 1173 (1999).
[9] S. Alonso, M. Bar, and R. Kapral, J. Chem. Phys. **133**, 214102 (2009).
[10] I. Mitkov, Physica D **133**, 398 (1999).
[11] J. M. Beck and V. Volpert, Physica D **182**, 86 (2003).
[12] S. Goroshin, F. D. Tang, and A. J. Higgins, Phys. Rev. E **84**, 027301 (2011).
[13] F. D. Tang, A. J. Higgins, and S. Goroshin, Combust. Theor. Model. **13**, 319 (2009).
[14] N. Provatas, T. Ala-Nissila, M. Grant, K. R. Elder, and L. Piché, Phys. Rev. E **51**, 4232 (1995).
[15] S. A. Rashkovskii, Combust. Explo. Shock. **41**, 35 (2005).
[16] S. K. Park and K. W. Miller, Commun. ACM **31**, 1192 (1988).
[17] In a continuum, two semi-infinite domains brought together at two different temperatures and the same heat capacity will reach an equilibrium temperature equal to the average of the two temperatures. This means that a semi-infinite domain initialized to T_{ad} via an imposed constant-volume reaction will only be able to initiate a reaction in the adjacent semi-infinite domain if its ignition temperature is half the adiabatic flame temperature $T_{\mathrm{ig}} = T_{ad}/2$. Thus, the initiating region must always be overdriven by a factor of at least twice the ignition temperature in order to initiate a front.
[18] M. D. Rintoul and S. Torquato, J. Phys. A **30**, L585 (1997).
[19] I. Sendiña-Nadal, A. P. Muñuzuri, D. Vives, V. Pérez-Muñuzuri, J. Casademunt, L. Ramírez-Piscina, J. M. Sancho, and F. Sagués, Phys. Rev. Lett. **80**, 5437 (1998).
[20] H. Hinrichsen, Braz. J. Phys. **30**, 69 (2000).
[21] P. Grassberger, in *Nonlinearities in Complex Systems, Shimla, 1995*, edited by S. Puri and S. Dattagupta (Narosa Publishing, New Delhi, 1997).